e-Prime - Advances in Electrical Engineering, Electronics and Energy 4 (2023) 100156

Contents lists available at ScienceDirect

e-Prime - Advances in Electrical Engineering, Electronics and Energy

journal homepage: www.elsevier.com/locate/prime

Contingency constrained TCSC and DG coordination in an integrated transmission and distribution network: A multi-objective approach

Ahmad Abubakar Sadiq [*,a,b], Muhammad Buhari [b], James Garba Ambafi [a], Sunusi Sani Adamu [b], Mark Ndubuka Nwohu [a]

[a] Department of Electrical and Electronic Engineering, Federal Univeristy of Technology, Minna, Nigeria
[b] Department of Electrical Engineering, Bayero Univeristy, Kano, Nigeria

ARTICLE INFO

Keywords:
Distributed generation
Contingency
Coordination
Multi-objective
Transfer capability
Thyristor control series compensator

ABSTRACT

Transmission System Operators (TSO) deploy Flexible AC Transmission Systems (FACTS) for congestion management in order to meet technical and multilateral power supply transactions. These power commitments are however constrained by thermal, voltage and stability limitations. On the other hand, the campaign to decarbonize the power supply framework as seen Distribution System Operators (DSO) accommodate an increased penetration of Distributed Generation (DG) within their distribution networks. However, prerogative of system operators for separate planning of FACTS and DG systems can worsen power system's key performance indicators especially under huge load growth and severe contingencies. Therefore, this paper developed an approach for contingency constrained coordination of Thyristor Controlled Series Compensator (TCSC) and DG through a multi-level optimization, comprising of a hybrid real power flow index and particle swarm in the first level and a multi-objective variant of particle swarm optimization in the second level. The contingency constrained coordination aimed to improve Available Transfer Capability (ATC), power loss and voltage deviation. Two models of DG were coordinated with TCSC under normal and contingency cases. Results indicate that while ATC improvement for various transactions were achieved with TCSC, additional power losses incurred was further reduced with DG deployment in coordination with TCSC. Furthermore, the Pareto front, which establishes the correlation between objectives shows a diving parabola that is partly nonlinear. Also, the $TCSC - DG_{PQ}$ provide superior ATC and power losses compared with $TCSC - DG_{PV}$. Again, under $(N-1)$ contingencies, the $TCSC - DG_{PQ}$ provides improved ATC compared with other contingency cases under TCSC only.

1. Introduction

Globally, dependence of human activities on electrical energy is rising steadily, and led to exponential growth in its demand under deregulation. However the load centres, are located far from the generation sources, which necessitate bulk power transfers such as multilateral transactions. This remains a common feature of a deregulated electricity market. The competitive framework of deregulation involving multilateral bids with increased demand causes tie lines to operate closer to and sometimes above transfer limits - thermal, voltage and stability [1–3]. Operating tie lines at their limits have caused network congestion, huge losses, poor voltage profile, and instability [4], with cascading impacts on the low voltage Distribution Networks (DN) [5].

In order to manage network operational performance and stability, the Transmission System Operators (TSO) must relieve congestion while meeting technical and multilateral supply commitments. Among the solutions adopted to enhance the static and dynamic performance of

Abbreviations: ATC, Available Transfer Capability; CPF, Continuation Power Flow; D-TCSC, Distributed TCSC; DER, Distributed Energy Resources; DG, Distributed Generation; DN, Distribution Networks; DSO, Distribution System Operators; FACTS, Flexible AC Transmission Systems; iT & DN, integrated Transmission and Distribution Network; MOO, Multi-Objective Optimization; MOPSO, Multi-Objective Particle Swarm Optimization; N - 1, Single Line Outage; PI - PSO, Hybrid Peformance Index Particle Swarm Optimization; PIM, Power Injection Model; Ploss, Power Loss; RE, Renewable Energy; SC, Shunt Capacitors; SSSC, Static Synchronous Series Compensator; SVC, Static Var Compensators; T & DN, Transmission and Distribution Network; TCSC, Thyristor Controlled Series Compensator; TN, Transmission Networks; TSO, Transmission Systems Operators; VD, Voltage Deviation; WSCC, Western System Coordinating Council.

* Corresponding author.
E-mail address: ahmad.abubakar@futminna.edu.ng (A.A. Sadiq).

https://doi.org/10.1016/j.prime.2023.100156
Received 11 January 2023; Received in revised form 24 March 2023; Accepted 13 April 2023
Available online 18 April 2023

power systems, the Flexible AC Transmission System (FACTS) devices are favourable features of the Transmission Networks (TN) [6–8]. Different FACTS were deployed for Available Transfer Capability (ATC) [9–11], voltage stability [12], power losses [13,14], dynamic stability [15,16], and congestion management [4,6,8]. A cost effective series FACTS family which modifies the effective line reactance is the Thyristor Controlled Series Compensator (TCSC) [17,18]. In complementing FACTS' deployment, the drive to decarbonize power supply framework witnessed increased deployment and utilization of Renewable Energy (RE) based Distributed Generation (DG), at the DN [19,20]. Although the increased penetration of DG reduces environmental impact, the grid-connected mode presents complexities if not properly planned [21]. Thus, increased penetration of DG raises concerns about stable and reliable operation due to intermittency in irradiance. Other issues of DG penetration, such as low fault ride-through, high fault current, and low power quality, may get worsen by FACTS' control operations [22,23].

The Literature is replete with the benefits of FACTS and DG in power systems: enhanced voltage stability, minimising power loss, improving ATC, and power system's management close to operating points [24]. FACTS also provide economic benefits in cost savings from loss and fuel cost minimization [25]. However, the distinction between Transmission and Distribution Network (T & DN) planning, and by extension FACTS and DG, translate to the uncoordinated system operators. This lack of coordination can worsen power system's performance in the presence of growth in demand [9], and occurrence of contingencies. Hence, coordination between FACTS and DG under growing demand, and considering contingencies is scarcely addressed in the literature.

Structural changes in modern power systems and manifestation of active DN are largely attributed to penetration of DG units. Consequently, separate planning of T & DN are no longer favourable. Economic dispatch, a major issue in planning and operation, requires coordinating the resources available to the system operators. While TN planning concerns periodical location of new infrastructures such as FACTS; to meet the demand growth, DN planning targets the optimal location and sizes of the substations and DGs. Therefore, the modern framework enables DSO to provide services in coordination with TSOs for an inclusive benefit [26]. Thus, the need for coordination of resources between TSO and DSO from operational and planning perspectives becomes germane in modern power systems operations. The major highlights of this paper are:

- Developed composite severity index for transmission line outage contingency, accounting for both power flows and bus voltages.
- Developed a contingency constrained approach for coordination of TCSC and DG thereby improving ATC, reducing power losses and voltage deviation.
- Establishes correlation between ATC Versus Power loss and ATC Versus Voltage deviation, under both normal and contingency conditions.

2. Literature review

Since flexibility in operations is an important condition for modern power systems dominated by renewable generation sources, [27] proposed a model to find the optimal mix of transmission-level assets such as Battery Energy Storage (BES), TCSC, and transmission lines. However, the work is limited to TSO planning and operations, while ignoring the impact of contingency conditions and interaction with DSO. Consequently, [28] demonstrated the integration of BES with PV as a DSO's flexible service in Radial Distribution System (RDS), though without a TSO to access this service. In [29] the importance of computing the feasible operating region between DSO and TSO to establish interconnection and without disturbing the stability of grid itself is emphasized. The importance of TSO - DSO cooperation is attributed to increasing penetration of intermittent and distributed energy resources in the distribution systems [30]. Three coordination schemes for TSO - DSO interactions where analyzed in [31].

The focus of review by Lind et al. [32] on the TSO - DSO coordination, is on the provision of balancing and congestion management services. Three out of the four key elements identified for TSO - DSO coordination are DER flexibility integration, coordination schemes and transmission-distribution optimization. The review also identifies technical barriers for optimizing a transmission-distribution grid as well as DER's flexibility to participate in grid services. Although the impacts of transmission assets on distribution network and performance of these asset under contingencies were ignored, [27] argued that flexibility has become important for modern power systems dominated by renewable generation sources. Hence the need to obtain an optimal mix of transmission-level non-generation flexible assets, such as Battery Energy Storage (BES), TCSC, and transmission lines. Similarly, [33] identifies exchange of reactive power at the interface between distribution and transmission systems as an importance issue due to ongoing relocation of generators to lower voltage levels. A flexibility measure is therefore proposed which describe the distribution system's capability to provide flexible reactive power exchange and the transmission system's needs to use these flexibilities. Although [27,32,33] presented the need for resources sharing in TSO - DSO coordination, impacts of contingencies were ignored in the overall coordination of resources.

A hierarchical framework to optimize TSO and DSO coordination is presented in [34]. It is argued in [35] that DG and TCSC intergration into a power system provides the grid with impressive technological and economic benefits. Concurrently, the discordance of DSO resource such as DG planning, ignoring active DN due to high DG penetration has been demonstrated to have adverse effects in [5], while the ability of TCSC to dampen oscillation is demonstrated in [36]. In [37–39], TCSC is deployed to improve power grid's performance in terms of ATC and loadability enhancement respectively. However, all ignored contingency, and without a distinction between transmission and distribution network. Accordingly, coordination between TSO and DSO is critical to optimize the benefits of FACTS and DG planning. The basic concern in TSO - DSO coordination is the ability of DSO to deploy its resources, to provide services to TSO [40]. Moreover, the TSO - DSO coordination environment must depict the features of a Transmission and Distribution Network (T & DN). Consequently, the model of an integrated Transmission and Distribution Network (iT & DN) is necessary, combining both the high and medium voltage sections [41–43]. Generally, services provided between TSO and DSO can be described in terms of technical key power system's performance indicators which FACTS and DGs planning seek to improve.

The works in [1,44] acknowledged that high penetration of DG causes reactive power demand, voltage instability, congestion, harmonics, power losses and other imbalances. Therefore, to avoid system-wide impacts, installing compensator such as TCSC, SVC, and STATCOM is necessary, to mitigates the impacts of DG. In [2,45,46], the optimal placement of TCSC with DG and Electrical Energy Storage (EES) are presented to manage congestion from load growth and line outages respectively. However, the impacts of DG or EES on FACTS and vice-versa, and lack of distinction between T & DN were ignored. Similarly, planning of DG with TCSC and Distributed TCSC (D-TCSC) for power loss reduction is presented in [14] and [47] respectively. In addition to single objective, [14] is limited to DN, while [47] ignores contingency and TSO - DSO interactions. Furthermore, the coordination of DG, Shunt Capacitors (SC) and Static Var Compensators (SVC) was presented in [9,13]. While [13] compares DG - SVC with DG - SC, only power loss reduction is considered as objective. In addition to power loss, [9] discussed the DG - SVC coordination to enhance ATC in a multi-objective approach. However, both ignored the distinction between TSO and DSO and impacts of contingency. To mitigate the uncertainty caused by DG, [25] combined the reactive power, transmission expansion, and TCSC planning to minimize investment costs of transmission lines, reactive power sources, and TCSC devices.

Furthermore, [38] presented the integration of Wind Energy (WE)

and FACTS. Optimal placement and size of Doubly-Fed Induction Generator (DFIG) based WE with two FACTS controller, viz. TCSC and Static Var Compensator (SVC) was demonstrated, and aimed at maximizing system loadability and minimize active power loss by satisfying various safety and stability constraints. While contingency was not considered, the test network is also limited to transmission network. Similarly, multiple DG and FACTS such as TCSC and STATCOM were optimally placed simultaneously without coordination of their impacts in [48]. Again, impact of contingency is ignored and the results are demonstrated in transmission network.

In [24], a multi-objective Tabu search algorithm is used for simultaneous planning of FACTS and DG unit in a distribution network. Both effect of transmission network and impact of contingency were ignored. In addition to the none optimal solution due to the analytical approach, there is no distinction between TSO and DSO of the modern competitive framework. In the same vain, to improve the technical and economic indices, a Multi-Objective Particle Swarm Optimization (MOPSO) is utilized to optimally place TCSC in [37,45,49]. While [37,45,49] ignores DG and the impact of contingencies, [37] considers only ATC enhancement with TCSC, [45] optimally place TCSC and Electrical Energy Storage (EES) and [49] uses fuzzy decision to select one of the Pareto-optimal solutions as the best compromise. Similarly, a multi-objective biogeography-based optimization (MOBBO) algorithm is used in [50] to optimally plan Static Synchronous Series Compensator (SSSC) in the wind integrated network.

Therefore, from the reviewed literature, separate planning of TCSC and DG were targeted at the T & DN respectively, to improve various objectives. However, the planning of TCSC and DG often ignored the imminent impacts of TCSC control operations on DG and provision of DG services for power flows and voltage control to TSOs, particularly under contingencies. Furthermore, power system operations involve monitoring multiple performance indices, hence multi-objective problem formulation. Consequently, this paper developed a contingency constrained approach for coordination of TCSC and DG thereby improving ATC, reducing power losses and voltage deviation.

3. Contingency constrained TCSC - DG coordination approach

The consideration of DN to facilitate effective provision of services to the TN is an important factor in TSO - DSO planning [51]. In this paper, the proposed TSO - DSO planning scenario depicts the TSO managed model, a fully centralized dispatch model, accounting for T & DN constraints [42,51]. In the contingency constrained $TCSC-DG$ coordination model depicted in Fig. 1, and operated by the TSO, is such that the resources available to both transmission and distribution levels are deployed and managed by the TSO in a coordinated manner for inclusive benefit.

From Fig. 1, the TSO section **A**, describes the first and inner level optimization using the hybrid $PI-PSO$ documented in [10], which is herein improved to consider single (N 1) line outage contingencies. The TSO section optimizes TCSC planning, thereby accounting for line outage. Using the Power Injection Model (PIM) of TCSC, inner optimization takes a set of candidate locations of TCSC obtained by the PI sensitivity. These candidates, with randomly generated sizes are used to explore and exploit the reduced search space, for an optimal ATC. The outer optimization takes the solution as input.

Similarly, the DSO section **B** is the second and outer level optimization which implement DG planning in coordination with contingency constrained TCSC planning. The outer optimization fixed the location of TCSC earlier obtained while optimizes the key performance indicators of ATC, P_{loss} and V_D using TCSCs size, location and size of DG as control variables. The $TCSC-DG$ contingency constrained coordination solutions for several power transfer transactions are obtained in section **C** of Fig. 1 by a 3-dimensional Pareto front plot.

3.1. Composite severity index for $(N-1)$ line outage contingency

A composite severity index for transmission line outage, a function of apparent power flow and voltage limit violations, is developed to measure the impacts of a given single line $(N-1)$ outage contingency. Equation (1) describe the performance index of the composite mth line outage contingency given as $PI^{m}_{S-V}(N-1)$.

$$PI^{m}_{S-V}(N-1) = f\left(f_p(x), f_v(x)\right) \tag{1}$$

In Eq. (1) x is a vector of the state variables (voltage magnitude and angle). $f_p(x)$ is the apparent power flow performance index defined by Eq. (2), where ω_m is a real non-negative weight coefficient that reflects the importance of the line, P_{lm} is active power flow, P^{rated}_{lm} is maximum allowable active power flow through the line, n is integer exponent.

$$f_p(x) = \sum_{m=1}^{Nl} \frac{w_m}{2n}\left(\frac{P_{lm}}{P^{rated}_{lm}}\right)^{2n} \tag{2}$$

Equations (3) and (4) give two variants of the voltage index measure of line outage performance index $f_p(x)$.

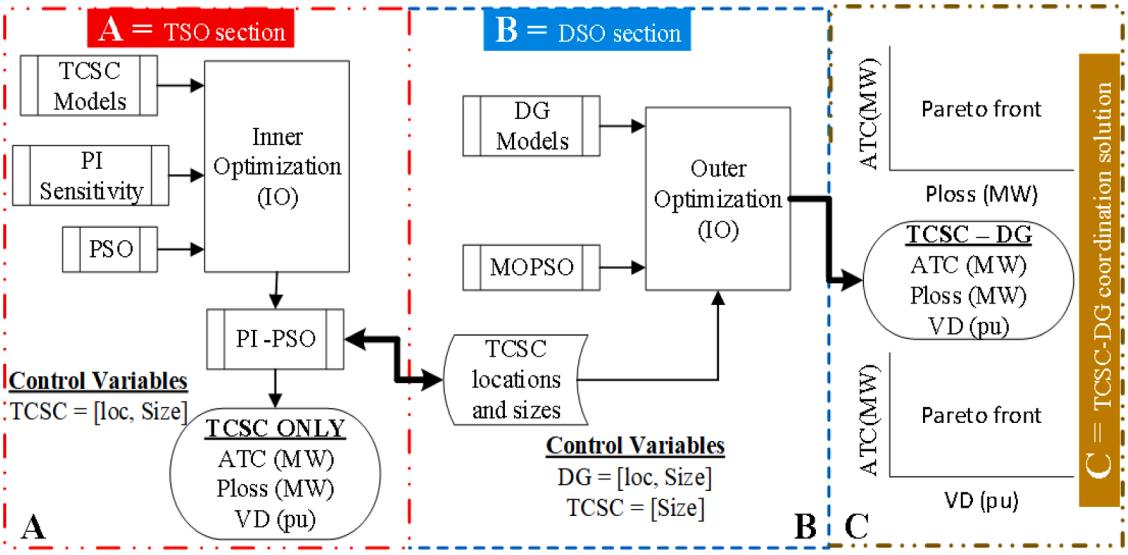

Fig. 1. $TCSC-DG$ Coordination Model.

$$f_v(x)_1 = \sum_{i=1}^{nb} \frac{\omega_i}{2} \frac{\Delta V_i}{\Delta V_i^{\lim}} \tag{3}$$

$$f_v(x)_2 = \sum_{i \in V_{vio}} \frac{\left|V_i - V_i^{\lim}\right|}{V_i^{\lim}} \tag{4}$$

From Eqs. (3) and (4), nb and ω_i are the number of buses and weight coefficient respectively, while Eqs. (5) and (6) define the terms ΔV_i, ΔV_i^{lim} and V_i^{lim} of Eqs. (3) and (4); which are change in ith bus pre and post contingency voltage, weighted difference of allowable voltage range and maximum or minimum voltage limit depending on the violation, respectively.

$$\left.\begin{aligned} \Delta V_i &= V_i - V_i^{sp} \\ \Delta V_i^{\lim} &= 0.5 \times \left(V_i^{\max} - V_i^{\min}\right) \end{aligned}\right\} \tag{5}$$

$$V_i^{\lim} = \begin{cases} V_i^{\max} & if\ V_i > V_i^{\max} \\ V_i^{\min} & if\ V_i < V_i^{\min} \end{cases} \tag{6}$$

V_i and V_i^{sp} are the post and pre contingency voltage magnitude at the ith bus, $V_i^{\min}$ and $V_i^{\max}$ are upper and lower voltage limits. Also, in Eq. (4) V_{vio} defines the set of all buses with post contingency voltage violation.

Equation (7) gives the simplified form of Eq. (1) with the two voltage variant, respectively. The outage of a transformer branch that causes a generator outage are excluded. In the TSO section **A**, the contingency constrained coordination of TSO DSO is obtained by firstly computing the composite severity index sub-block using Eq. (7). Where S_{lm} is the post contingency apparent power flow of a given line.

$$PI_{S-V}^{m}(N-1) = \begin{cases} \sum_{m=1}^{Nl} \frac{w_m}{2n} \left(\frac{S_{lm}}{S_{lm}^{rated}}\right)^{2n} + \sum_{i=1}^{nb} \frac{\omega_i}{2} \frac{\Delta V_i}{\Delta V_i^{\lim}} \\ \text{OR} \\ \sum_{m=1}^{Nl} \frac{w_m}{2n} \left(\frac{S_{lm}}{S_{lm}^{rated}}\right)^{2n} + \sum_{i \in V_{vio}} \frac{\left|V_i - V_i^{\lim}\right|}{V_i^{\lim}} \end{cases} \tag{7}$$

4. Multi-objective optimization (MOO) problem formulation

Power systems planning studies often target multiple objectives, which sometimes are contradictory [52]. Due to multi-objectives, the search space is not always well defined, hence the need for a Multi-Objective Optimization (MOO), which has no absolute global best, but some set of non-dominated solutions. In MOO, the objectives may not have a direct correlation. A general minimization formulation is expressed in Eq. (8), subject to equality and inequality constraints of Eqs. (9) and (10). Equation (9) describes the compact power flow problem to be solved. While Eq. (10) is the TCSC control parameter, which models the TCSC's size as bounded by lower and upper limit ($Xc^{\min}$ and $Xc^{\max}$) respectively.

$$\text{minimize } \overrightarrow{f}(x,\lambda) = [f_1(x,\lambda), f_2(x,\lambda) \ldots f_m(x,\lambda)] \tag{8}$$

$$f(x,\lambda) = 0 \tag{9}$$

$$X_c^{\min}(x,\lambda) \le X_c(x,\lambda) \le X_c^{\max}(x,\lambda) \tag{10}$$

In Eqs. (8) to (10), x and λ are vector of state and control variables, and the Pareto optimal approach is applied to the problem of Eq. (8), according to dominance model. For a problem having m objectives, a solution (x_i, λ_i) dominates other solution (x_j, λ_j), if (x_i, λ_i) is better than (x_j, λ_j) for at least one objective $\overrightarrow{f_i}(x,\lambda)$, and is not worse for any other $\overrightarrow{f_j}(x,\lambda)$, as described in Eq. (11). Where $j = 1, 2 \ldots m$ and $j \neq i$. The symbol $\succ$ in Eq. (11) represents the domination concept. In a non-dominated pair, an improvement in objective $\overrightarrow{f_i}(x,\lambda)$ can cause the deterioration of other objectives [50].

$$\left.\begin{aligned} &\overrightarrow{f_i}(x_1,\lambda_1) < \overrightarrow{f_i}(x_2,\lambda_2) \\ &\text{and} \\ &\overrightarrow{f_j}(x_1,\lambda_1) \le \overrightarrow{f_j}(x_2,\lambda_2) \end{aligned}\right\} \Rightarrow (x_1,\lambda_1) \succ (x_2,\lambda_2) \tag{11}$$

4.1. ATC-objective Using continuation power flow (CPF)

MOO can exist in two fronts, either as minimization and maximization, hence the need to transform to the same front. At the maximum power transfer limit imposed by thermal, voltage, and generator reactive power [10], the ATC evaluate to Eq. (12).

$$\text{Max.}\left\{\sum_{i \in \sin k} P_L^i(\lambda = \lambda_{lim}) - \sum_{i \in \sin k} P_L^i(\lambda = 0)\right\} \tag{12}$$

For the contingency constrained TCSC DG coordination, Eq. (12) is subject to nonlinear power flow equations as well as Eq. (7) which computes the feasible (N - 1) contingencies. Negating the ATC term of Eq. (12), transform the problem formulation to minimisation front.

4.2. Power loss-Objective

Equation (13) expresses the real power loss of an integrated power system comprising the T & DN losses. Where g_k is the conductance of transmission line. V_i, V_j, δ_i, δ_i are the voltage magnitudes and angles at buses/nodes i and j respectively, nl is the number of lines in the network.

$$P_{loss}^{net} = P_{loss}^{TSO} + P_{loss}^{DSO} \tag{13a}$$

$$P_{loss}^{net} = \sum_{k=1}^{nl} g_k \left(V_i^2 + V_j^2 - 2V_iV_j\cos\left(\delta_i - \delta_j\right)\right) \tag{13b}$$

4.3. Voltage deviation-objective

Ideally, every bus/node voltage is desired at 1p.u. However, excess load demand or switching surges may result into under or over voltages away from 1p.u. The concept of voltage deviation herein measures how far a given voltage is, from its ideal value of 1p.u. Consequently, at each bus/node, the deviation of voltage magnitudes away from 1p.u., measures the quality of voltage at such bus/node. Thus, the absolute sum of voltage deviation of all bus/nodes in the network is taken as a measure of the network's overall quality of voltage supply expressed by Eq. (14).

$$V_D^{net} = V_D^{TSO} + V_D^{DSO} = \sum_{i=1}^{nb} |1 - V_i| \tag{14}$$

Equation (15) describes the set of fitness vector comprising: ATC, P_{loss}^{net} and V_D^{net}, for the contingency constrained $TCSC - DG$ coordination.

$$\overrightarrow{f}(x,\lambda) = \begin{cases} -ATC \\ P_{loss}^{net} = P_{loss}^{TSO} + P_{loss}^{DSO} \\ V_D^{net} = V_D^{TSO} + V_D^{DSO} \end{cases} \tag{15}$$

5. Component modelling

5.1. TCSC power injection model (PIM)

The pie equivalent model of a transmission line with TCSC jx_c is given in Fig. 2. The equivalent line reactance with TCSC is given by the Eq. (16), while the active and reactive power flows with TCSC are expressed by the Eqs. (17)–(22).

$$X_{ij}^{equ} = X_{ij} + jx_c \tag{16}$$

$$P_{ij} = V_i^2 G_{ij}^{'} - V_iV_j\left(G_{ij}^{'}\cos\delta_{ij} + B_{ij}^{'}\sin\delta_{ij}\right) \tag{17}$$

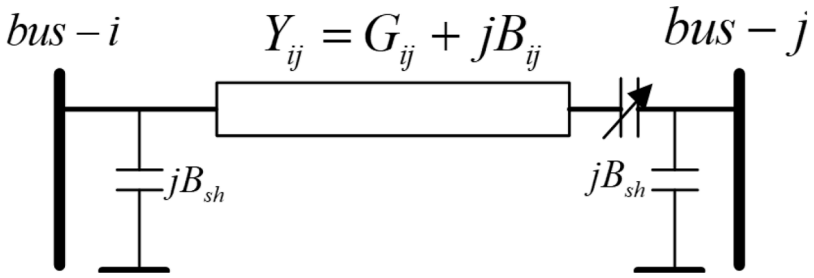

Fig. 2. Transmission line Model with TCSC.

$$Q_{ij} = -V_i^2\left(B_{ij}^{'} + B_{sh}\right) - V_iV_j\left(G_{ij}^{'}\sin\delta_{ij} - B_{ij}^{'}\cos\delta_{ij}\right) \tag{18}$$

$$P_{ji} = V_j^2G_{ij}^{'} - V_jV_i\left(G_{ij}^{'}\cos\delta_{ij} - B_{ij}^{'}\sin\delta_{ij}\right) \tag{19}$$

$$Q_{ji} = -V_j^2\left(B_{ij}^{'} + B_{sh}\right) + V_jV_i\left(G_{ij}^{'}\sin\delta_{ij} + B_{ij}^{'}\cos\delta_{ij}\right) \tag{20}$$

$$G_{ij}^{'} = \frac{r_{ij}}{r_{ij}^2 + \left(x_{ij} - x_c\right)^2} \tag{21}$$

$$B_{ij}^{'} = \frac{-\left(x_{ij} - x_c\right)}{r_{ij}^2 + \left(x_{ij} - x_c\right)^2} \tag{22}$$

From Fig. 2, using the PIM Model, the effect of TCSC's series reactance on active power flow is represented by equivalent power injections at receiving and sending end of the line without TCSC [53], as shown in Fig. 3. Equations (23) and (24) give the real power injections at both ends of Fig. 3, while Eqs. (25) and (26) give the change in conductance and susceptance, respectively.

$$P_{ic} = V_i^2\Delta G_{ij} - V_iV_j\left(\Delta G_{ij}\cos\delta_{ij} + \Delta B_{ij}sin\delta_{ij}\right) \tag{23}$$

$$P_{jc} = V_j^2\Delta G_{ij} - V_jV_i\left(\Delta G_{ij}\cos\delta_{ij} - \Delta B_{ij}sin\delta_{ij}\right) \tag{24}$$

$$\Delta G_{ij} = \frac{x_cr_{ij}\left(x_c - 2r_{ij}\right)}{\left(r_{ij}^2 + x_{ij}^2\right)\left(r_{ij}^2 + \left(x_{ij}^2 - x_c\right)^2\right)} \tag{25}$$

$$\Delta B_{ij} = \frac{-x_c\left(r_{ij}^2 - x_{ij}^2 + x_cx_{ij}\right)}{\left(r_{ij}^2 + x_{ij}^2\right)\left(r_{ij}^2 + \left(x_{ij}^2 - x_c\right)^2\right)} \tag{26}$$

5.2. DG Modelling

Based on DG's ability to inject real and reactive power [54,55], two DG models are implemented [56–59].

1. **PV Model:** DG supplies only real power.
2. **PQ Model:** DG supplies real and reactive power.

DGs are modelled as negative load [56] when the dynamics and fast transients associated with converter-based DG are neglected. Accordingly, if P_{li} and Q_{li} represent the real and reactive load at the ith node of a DN, Eqs. (27) and (28) describe the new loads (P_{nli}, Q_{nli}) after DG integration; where γ_{dg}^{p} and γ_{dg}^{q} are real and reactive power injections from DG units.

$$P_{nli} = P_{li} - \gamma_{dg}^{p} \tag{27}$$

$$Q_{nli} = Q_{li} - \gamma_{dg}^{q} \tag{28}$$

Equations (27) and (28) imply that DG units replace a certain amount of load demand at the said DN's node and is subject to the power balance Eqs. (29) and (30).

$$P_G^i - P_L^i - P_{inj}^i = 0 \tag{29}$$

$$Q_G^i - Q_L^i - Q_{inj}^i = 0 \tag{30}$$

The power injections P_{inj}^i and Q_{inj}^i is described by Eqs. (31) and (32) respectively; where P_G^i, Q_G^i, P_L^i, Q_L^i are real and reactive generation and load at the ith node.

$$P_{inj}^i = \sum_{j=1}^{n} V_iV_jY_{ij}\cos\left(\delta_i - \delta_j - \theta_{ij}\right) \tag{31}$$

$$Q_{inj}^i = \sum_{j=1}^{n} V_iV_jY_{ij}\cos\left(\delta_i - \delta_j + \theta_{ij}\right) \tag{32}$$

DG penetration level stipulates the limit of real or reactive power supply from DG, and the Eq. (33) defines penetration level [54].

$$\sum_{i=1}^{ndg} PQ_{dg}^i \le \mu \sum_{j\in PQ_{load}} PQ_{load}^j \tag{33}$$

In the Eq. (33), the total real or reactive power injected by DG is a percentage of the DN real or reactive power demand; hence, the penetration level is μ. The inequality constraint described by Eq. (10), limits the maximum real and reactive from DG to 75% of PQ_{load} load in DN [60–62] as described by Eqs. (34) and (35).

$$0 \le \gamma_{dg}^{p} \le 0.75P_{load}^{dn} \tag{34}$$

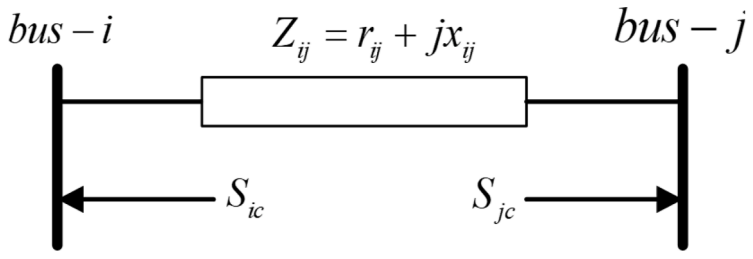

Fig. 3. Power Injection Model of TCSC.

$$-0.75Q_{load}^{dn} \le \gamma_{dg}^{q} \le 0.75Q_{load}^{dn} \quad (35)$$

6. Reduced search space

Since power flows and overloads are major constraints to ATC [63], the sensitivity of real power flow to TCSC's reactance is used to obtain the list of candidate lines for TCSC location [64].

6.1. Real power flow sensitivity

The sensitivity of real power flow in a line where TCSC is located can be expressed in terms of partial derivatives of the power injection in terms of Eqs. (23) and (24), as expressed by Eqs. (36) and (37), respectively [53].

$$\left.\frac{\partial P_i}{\partial X_k}\right|_{x_k=0} = \left.\frac{\partial P_{ic}}{\partial X_k}\right|_{x_k=0} = \left(V_i^2 - V_i V_j \cos\delta_{ij}\right)\left.\frac{\partial \Delta G_{ij}}{\partial X_k}\right|_{x_k=0} - \left(V_i V_j \sin\delta_{ij}\right)\left.\frac{\partial \Delta B_{ij}}{\partial X_k}\right|_{x_k=0} \quad (36)$$

$$\left.\frac{\partial P_j}{\partial X_k}\right|_{x_k=0} = \left.\frac{\partial P_{jc}}{\partial X_k}\right|_{x_k=0} = \$V_j^2 - V_i V_j \cos\delta_{ij}\left.\frac{\partial \Delta G_{ij}}{\partial X_k}\right|_{x_k=0} + \left(V_i V_j \sin\delta_{ij}\right)\left.\frac{\partial \Delta B_{ij}}{\partial X_k}\right|_{x_k=0} \quad (37)$$

where,

$\left.\frac{\partial \Delta G_{ij}}{\partial X_k}\right|_{x_k=0} = 2G_{ij}B_{ij}$ and $\left.\frac{\partial \Delta B_{ij}}{\partial X_k}\right|_{x_k=0} = B_{ij}^2 - G_{ij}^2$

6.2. Hybrid real power flow sensitivity and PSO $(PI-PSO)$ for TCSC planning

Consequently, with the reduced search space constituting the candidate locations obtained by real power flow sensitivity, PSO is deploy to locate and size TCSC for ATC enhancement. The complete documentation of the hybrid real power flow sensitivity and PSO is given in [10].

Fig. 4 depicts flowchart of the developed multi-level optimization approach. The first and inner level is the hybrid real power flow performance index and particle swarm optimization (PI-PSO). the second and outer level implement the Multi-Objective Particle Swarm Optimization (MOPSO). From Figs. 1 and 4, the outer optimization depends on the output of the inner optimization which are the optimal solutions of the TCSC planning obtained by the PI - PSO.

7. Synthetic test network (iT & DN)

The power system test network is carefully selected to model an integrated Transmission and Distribution Network (iT & DN). The high voltage transmission section is the Western System Coordinating Council network (WSCC) at a nominal of 230 kV, while the IEEE 16 nodes form the distribution section at a nominal of 23 kV. Fig. 5 depicts the topology of iT & DN [5]. Fig. 5a shows the one-line diagram of iT & DN illustrating the point of common coupling between transmission and distribution sections, while Fig. 5b gives the entire topology of the modified test network with part of the loads at buses 5, 6 and 8 of the transmission section replaced by IEEE 16 nodes distribution network. The transmission section comprises of 3 generators with total output of 322 MW, 3 transformers and 6 transmission lines. The entire iT & DN comprises 9 buses and 48 nodes of transmission and distribution section respectively, numbered consecutively from 1 to 57. The total load demand is 315 MW. The developed approach for contingency constrained coordination of $TCSC-DG$ is implemented within MATLAB/MATPOWER environment [10]. Data exchange is between MATPOWER, which evaluate load flow and CPF, and MATLAB implementation of MOPSO. Table 1 gives PSO and MOPSO parameters.

8. Result and discussion

The various power transfer directions [10], are described in Table 2. The transfer direction comprises both bilateral and multilateral transactions. The 2^{nd} and 3^{rd} column of Table 2 outline the source and sink buses corresponding to each transaction. Additionally, the base case multiple objectives comprising the ATC, power losses and voltage deviation of the test network (iT & DN) are also shown in Table 2. From Table 2, the binding limitation to each transaction is specific to transfer direction, which is either branch apparent power flows for T1 to T10 or bus voltage constraints in the case of T11 to T13.

Using $PI-PSO$, the active power loss and voltage deviation corresponding to the enhanced ATC values with TCSC for transactions T1 to T10 are given in Table 3. The results in Table 3 are obtained such that the percentage compensation for TCSC is bounded within –

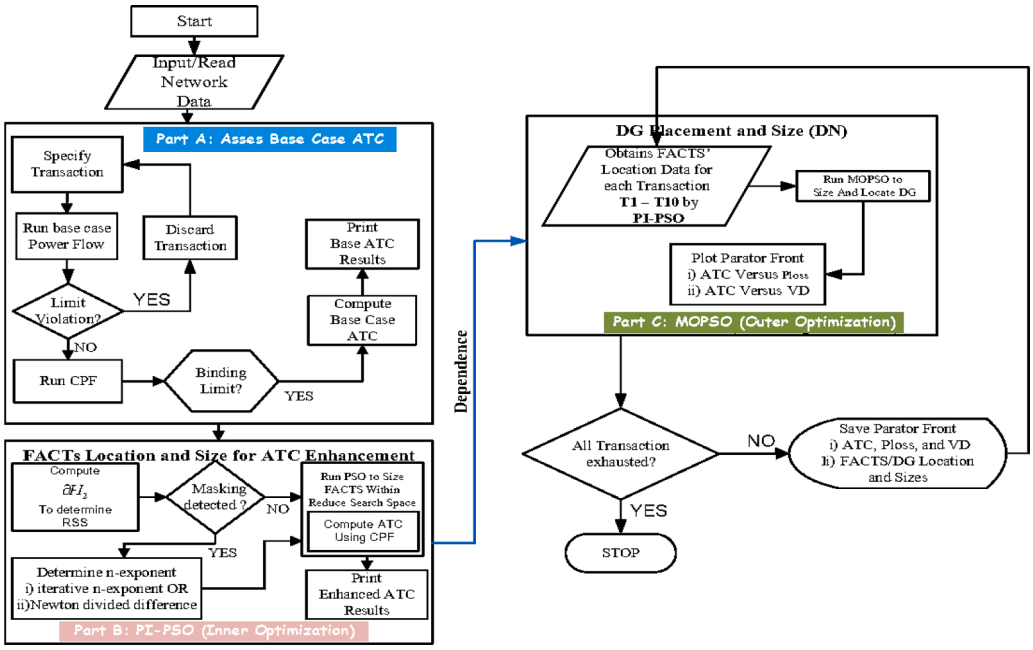

Fig. 4. Flowchart of the Developed Multi-Level Approach to TCSC - DG Coordination.

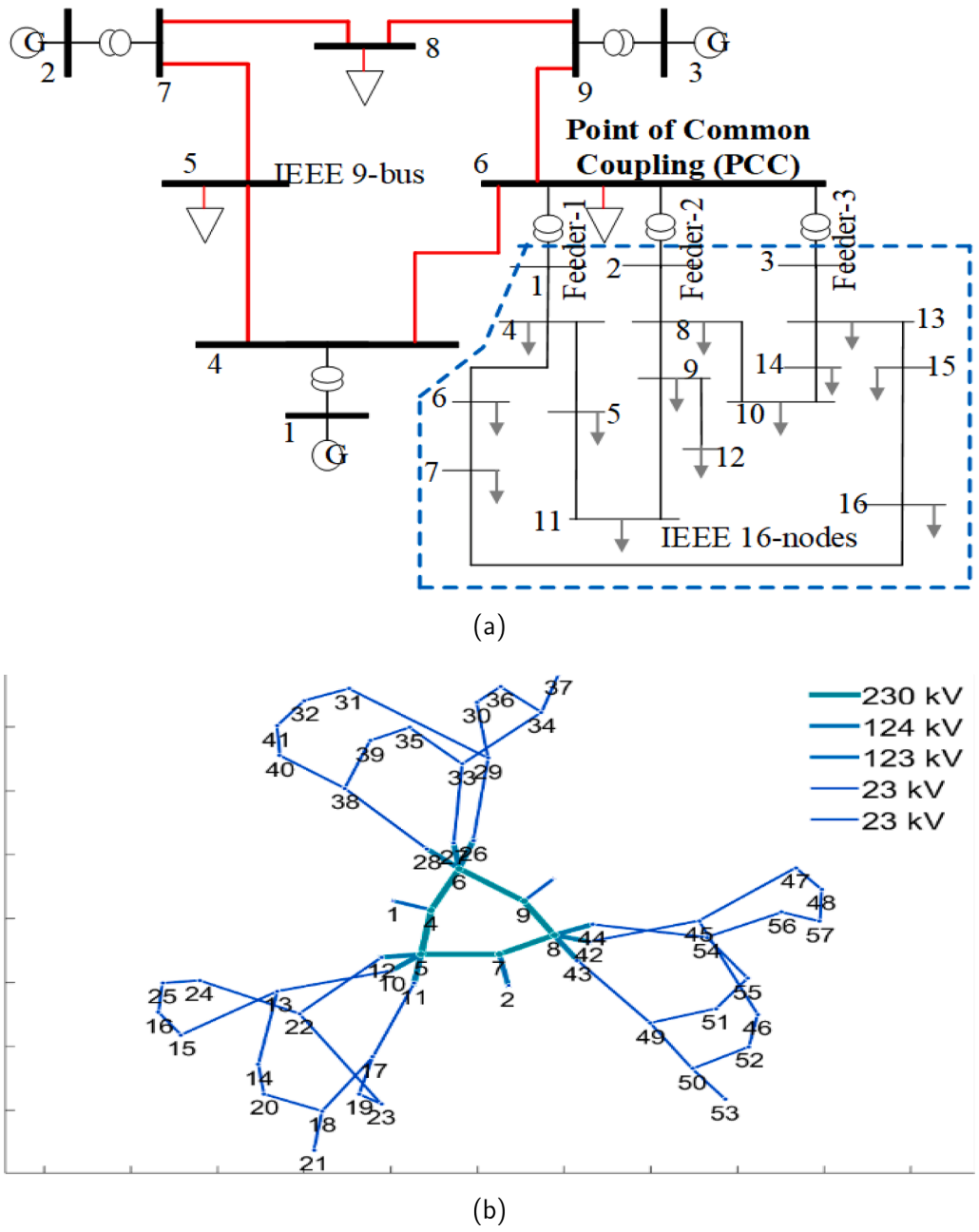

Fig. 5. Topology of the iT & DN. (a) One-line diagram (b) Entire topology of iT & DN.

Table 1
PSO and MOPSO Paramters.

Params.,	PSO	MOPSO	Params.,	PSO	MOPSO	Params.,	PSO	MOPSO
ω_o	0.9	0.5	C_1	1.5	1.0	C_2	$4 - C_1$	2
ω_{damp}	–	0.99	Max_{It}	150	150	$Swarm_{size}$	9	200
ω_{it}	$= 0.1 * \frac{it-1}{Max\_it-1}$	$= \omega_0 * 0.99$	Repos.,	–	100	Grids per Dim.	–	7
(α)	–	0.1	β	–	2	γ	–	2
(mu)	–	0.1	–	–	–	–	–	–

$0.2 \leq X_{TCSC} \leq 0.8$. The results obtained and their discussions are presented in four folds:

I A comparison of the objective (ATC, power loss and voltage deviation) without (base case) and with TCSC and no DG. This is presented by Tables 2, 3 and Fig. 6. It is established that while ATC enhancement with TCSC was observed, additional power losses were incurred due to increased power flows.

II Results of TCSC coordination with DG and a correlation among objectives are presented by Figs. 7, 8, and 9 as well as Tables 4 and 5. Also, a comparison between PV and PQ model of DG in

Table 2
Base Case ATC for Various Transactions of iT & DN test network.

Trans	Source	Sink	Loading	ATC		P_{loss}	V_D	Limiting
ID	Buses	Buses	Factor(λ_{max})	[p.u.]	[MW]	[MW]	[p.u.]	Element
T1	1,3	5	1.5761	1.41817	141.8172	6.2044	3.6935	3(5 to 7)
T2	1,2	5,8	0.6620	1.25676	125.6763	3.9991	2.6895	5(7 to 8)
T3	1,2,3	5,6	0.5520	1.18561	118.5608	3.7575	3.4024	3(5 to 7)
T4	1,2,3	6,8	0.6770	1.52260	152.2604	4.3310	3.7203	5(7 to 8)
T5	2,3	5	0.4860	0.43772	43.7716	2.5070	2.0115	3(5 to 7)
T6	1	8	1.2410	1.24089	124.0892	4.4390	2.2023	5(7 to 8)
T7	1,2,3	5,8	0.7380	1.40208	140.2082	4.4523	3.2861	3(5 to 7)
T8	2,3	6	0.6010	0.75099	75.0992	2.9377	3.0173	3(5 to 7)
T9	1,2	8	0.5950	0.59529	59.5292	2.6632	1.7187	5(7 to 8)
T10	1,2	5,6	0.7450	1.60236	160.2364	4.8511	4.2759	3(5 to 7)
			Voltage Constrained Transactions					
T11	1	6	0.9700	1.21272	121.2717	4.0264	3.0622	bus-6
T12	1,3	6	0.9320	1.16474	116.4743	3.9116	3.1138	bus-6
T13	1,2,3	5,6,8	0.7140	2.24809	224.8094	5.9844	4.8829	bus-6

Table 3
Enhanced ATC Values with TCSC using $PI - PSO$ for iT & DN.

Trans	ATC	P_{loss}	V_D	TCSC Solution	
ID	[MW]	[MW]	[p.u.]	Line No.	% Comp
T1	154.5033	6.7954	3.4577	8(9 to 6)	80
T2	153.4515	4.7291	3.044	3(5 to 7)	49.2712
T3	172.1144	5.0027	3.9008	8(9 to 6)	75.5499
T4	178.2661	5.0092	4.2383	3(5 to 7)	44.6538
T5	64.4571	3.052	2.3949	8(9 to 6)	80
T6	153.3719	5.5736	2.3356	9(6 to 4)	80
T7	151.2495	4.7096	3.2706	5(7 to 8)	53.965
T8	101.3858	3.5028	3.3194	8(9 to 6)	56.4783
T9	79.304	3.1254	2.1354	3(5 to 7)	68.1384
T10	171.4634	5.0718	4.1904	8(9 to 6)	34.4068

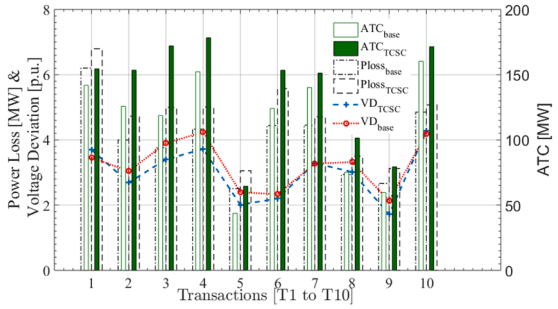

Fig. 6. Comparison of Objectives.

coordination with TCSC is provided by Figs. 8 and 9 and Tables 4 and 5.

III Impacts of single line ($N-1$) outage contingency on ATC enhancement with TCSC presented by Fig. 10. Earlier, contingency ranking results is presented in Table 6.

IV Finally, the impacts of DG coordination with TCSC under single line ($N-1$) outage contingency, on the three objectives, are presented and illustrated by Figs. 11, 12 and 13.

A comparison of the results of these objectives in Tables 2 and 3 is depicted in Fig. 6. Observed that while ATC enhancement with TCSC was recorded, there are corresponding active power losses resulting from additional power flows due to bilateral and multilateral transactions. Also, the voltage profile resulting from the transactions shows further deviation from the base case conditions. Hence, the need for coordinated approach between TSO and DSO, thereby ensuring better performance (measured by the objectives) of the iT & DN.

Accordingly, the $TCSC - DG$ coordination model described in Fig. 1 is implemented. Thus, for different transactions of Table 2, Fig. 7 shows the three dimensions (3D), non-dominated Pareto front of $TCSC - DG$ coordination, for the optimisation of ATC, active power loss, and voltage deviation with both PV and PQ models of DG. As indicated in Table 1, the Pareto front plots constitute the 100 members of the repository, which are the non-dominated solutions providing unique solutions among the competing objectives. It is observed that the 3D Pareto front in Fig. 7a to d indicates a diving parabolic like shape, which is partly nonlinear. Furthermore, to gain a clearer insight into the relationships among the competing objectives, the slices of the 3D Pareto front plot illustrating the correlation between any two of the competing objectives will establish a unique understanding of the relationship between: ATC versus Ploss, ATC versus V_D and Ploss versus V_D respectively.

The slices of the Pareto front are obtained from the 3D plots of Fig. 7a to d, thereby illustrating the correlation between any two objectives. For transactions T1 and T3, the Pareto plot slices of ATC against real power loss (Ploss) and ATC against voltage deviation (V_D) are given in Figs. 8 and 9 respectively. It is worthy to state here that the Pareto plot slices between Ploss and V_D depicts disorderliness and hence were not discussed further.

For the power transfer transaction illustrated in Figs. 8 and 9, the sub-figs. such as Fig. 8a and b depict the Pareto front slices with $TCSC - DG_{PV}$ while Fig. 8c and d depicts $TCSC - DG_{PQ}$ coordination. Similarly, Figs. 8a and c give the Pareto front slices for the correlation between ATC versus Ploss, whereas Fig. 8b and d gives the correlation between Pareto front of ATC versus V_D, respectively. In the case of $TCSC - DG_{PV}$, from Fig. 8a and c, it was observed that the Pareto front peaks with ATC, Ploss and V_D values around 168 MW, 6.2 MW and 3.8 p.u. as against 154.5 MW, 6.7 MW and 3.5 p.u respectively. These improvements are attributable to DSO's resources, such as DG in coordination with the TSO's TCSC.

For comparison and deeper insight into the non-dominated solutions, a two-level criterion is adopted to select one non-dominated solution as the optimum compromise of the three objectives. In the first level, the ATC enhancement is given priority, such that all solutions with higher ATC compared to TCSC only constitute the optimum solution. The second level criterion is based on the concept of dominance, and a member of the non-dominated solution with at least two superior objectives compared to TCSC only equally constitute the optimum solution. Finally, from the list of the optimum solutions, a non-dominated solution is selected as the optimal solution by applying the first level criteria again.

For transactions T1 to T10, Tables 4 and 5 gives the objective terms and the corresponding solutions for $TCSC - DG_{PV}$ and $TCSC - DG_{PQ}$ coordination, respectively.

In the case of Transaction T1, from Table 5, Fig. 8c and d, it is seen that the PQ model of DG, in coordination with TCSC (as in $TCSC - DG_{PQ}$), provide superior ATC values compared with the PV model of DG,

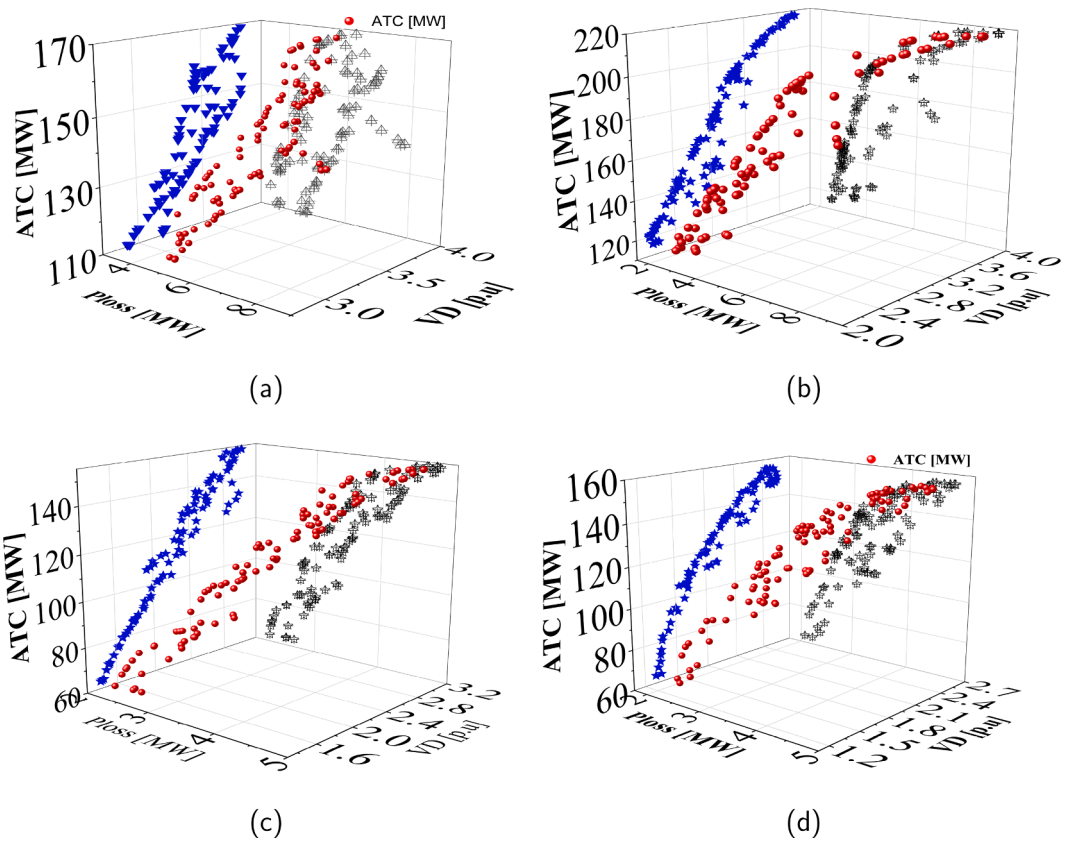

Fig. 7. Pareto front Plot of T1 with $TCSC - DG$. (a) T1 under $TCSC - DG_{PV}$ (b) T1 under $TCSC - DG_{PQ}$ (c) T2 under $TCSC - DG_{PV}$ (d) T2 under $TCSC - DG_{PQ}$.

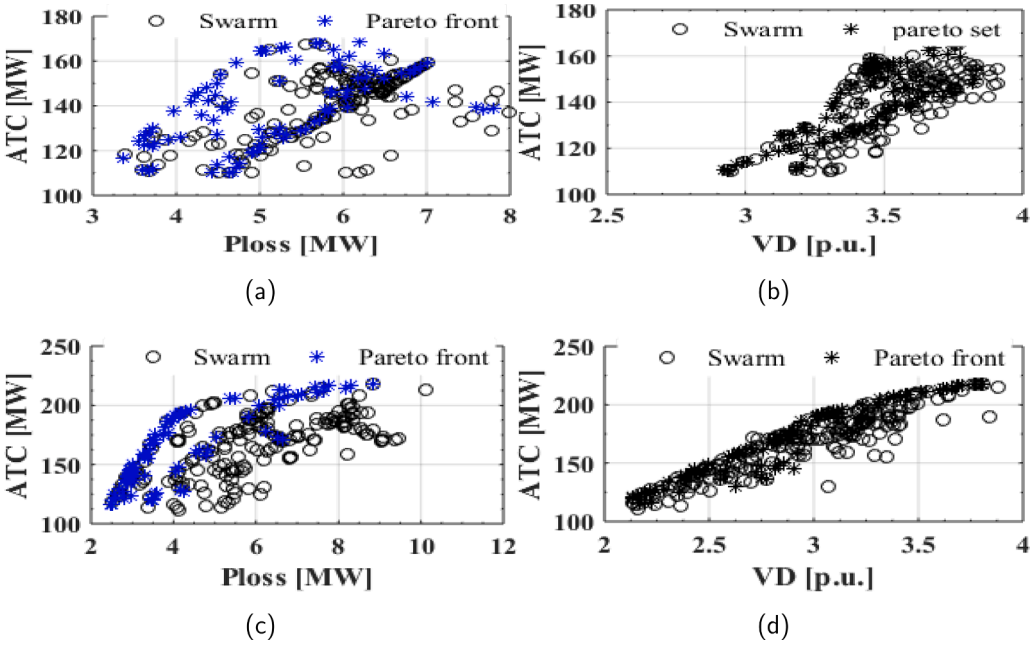

Fig. 8. Slices of Pareto plot for transaction T1 under $TCSC - DG$. (a) $TCSC - DG_{PV}$ (b) $TCSC - DG_{PV}$ (c) $TCSC - DG_{PQ}$ (d) $TCSC - DG_{PQ}$.

which is depicted by Table 4 and Fig. 8a and b. Also, for the ATC versus Ploss, such as illustrated in Fig. 9c and d, the Pareto slices indicate that at some maximum ATC, the slope of the Pareto front approaches zero, implying that additional power losses are incurred without a corresponding enhancement in ATC.

Furthermore, comparing the results of a given transaction, such as T1 with only TCSC given in Table 3, and T1 with $TCSC - DG$ coordination of Table 4 (with PV model of DG) or Table 5 (with PQ model of DG), it is observed that the DG planning (at the distribution section of iT & DN) in coordination with TCSC reduces the power loss below those of only TCSC. Thus, the impact of iT & DN is to ensure that the DSO resource which in this case is the DG, participate in grid service provision in terms

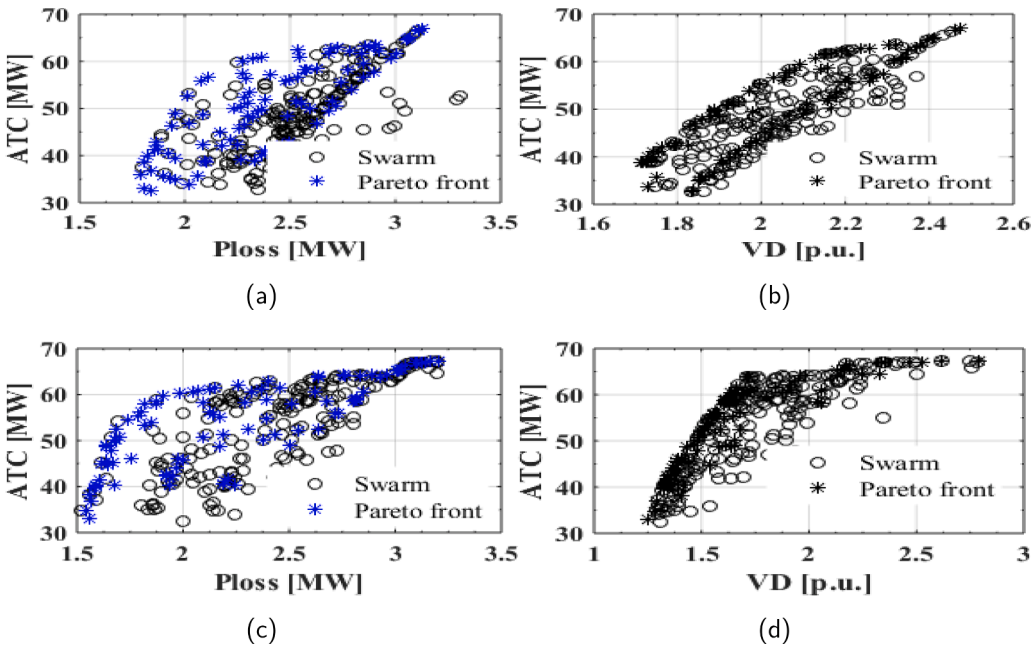

Fig. 9. Slices of Pareto plot for transaction T3 under $TCSC - DG$. (a) $TCSC - DG_{PV}$ (b)$TCSC - DG_{PV}$ (c) $TCSC - DG_{PQ}$ (d)$TCSC - DG_{PQ}$.

Table 4
$TCSC - DG_{PV}$ Coordination Solution for T1 to T10.

Trans	ATC [MW]		$TCSC - DG_{PV}$ Solution					
ID	TCSC	$TCSC - DG_{PV}$	$Ploss[MW]$	$V_D[p.u.]$	Line No.	% Comp.	Node No.	P_Size [MW]
T1	154.503	168.8304	6.206	3.8241	8(9 to 6)	80	21	3.9664
T2	153.452	153.5067	4.7252	3.0241	3(5 to 7)	48.9181	10	8.7171
T3	172.114	172.2701	4.8214	3.8249	8(9 to 6)	80	49	10.2293
T4	178.266	178.8987	4.999	4.1679	3(5 to 7)	25.6021	28	21.5
T5	64.4571	63.5931	2.9089	2.3187	8(9 to 6)	80	31	6.3847
T6	153.372	168.3154	4.7358	2.3954	9(6 to 4)	80	50	21.5
T7	151.25	151.6302	4.6989	3.2171	5(7 to 8)	80	42	11.9087
T8	101.386	101.5266	3.5288	3.11	8(9 to 6)	69.1184	48	21.5
T9	79.304	79.6278	2.9211	1.9826	3(5 to 7)	62.1141	36	14.7665
T10	171.463	169.5974	5.0629	4.1745	5(7 to 8)	68.3549	26	14.2134

Table 5
$TCSC - DG_{PQ}$ Coordination Solution for T1 to T10.

Trans	ATC [MW]		$TCSC - DG_{PQ}$ Solution						
ID -	TCSC -	$TCSC - DG_{PV}$	$Ploss$ [MW]	V_D [p.u.]	Line Numb.	Perc.% Comp.	Node Numb.	P_Size [MW]	Q_Size [MVAR]
T1	154.503	196.4656	4.4158	3.1387	8	80	18	11.2398	13
T2	153.452	155.3124	4.6795	2.4445	3	46.5784	56	0	13
T3	172.114	174.1671	4.5908	3.3141	8	68.634	18	0	12.9518
T4	178.266	183.2228	4.8576	3.7687	3	41.3541	45	0	12.9919
T5	64.4571	66.5036	3.0491	2.1733	8	80	11	19.7611	12.7953
T6	153.372	181.9170	3.6233	1.5008	9	80	50	21.5	13
T7	151.25	153.7433	4.685	2.7673	5	52.0642	56	0.2591	12.9781
T8	101.386	101.9827	3.0216	2.6511	8	54.8568	34	0	13
T9	79.304	80.9899	3.1235	1.9333	3	46.5589	44	15.6893	13
T10	171.463	173.9668	4.8871	3.8261	5	44.2909	14	0	10.9326

of real power loss reduction.

An important event considered in power systems planning and operations is the outage of the TSO's equipment, such as the transmission line. Therefore, in the TSO managed model, a single line outage $(N-1)$ contingency can illustrate the impacts of TSO's contingency on the integrated Transmission and Distribution Networks. Consequently, Table 6 gives the result of $(N-1)$ contingency based on Eq. (37). From the topology of Fig. 5, at the transmission section, the transformer branch outages are termed "Invalid" in Table 6, since it also results in the outage of a generator; while the "unfeasible" term refers to line outages that cause singularity and hence non-convergence of the load flow at the base case. In Table 6, PI_S, PI_{V1} and PI_{V2} are the apparent power version of the performance index, and the two voltage variant measurements of line outage performance index described by Eq. (37). The ranks of the outage lines based on the composite severity indices PI_{S-V1},PI_{S-V2} and PI_S are shown in **boldface**. From each severity indices shown in Table 6,

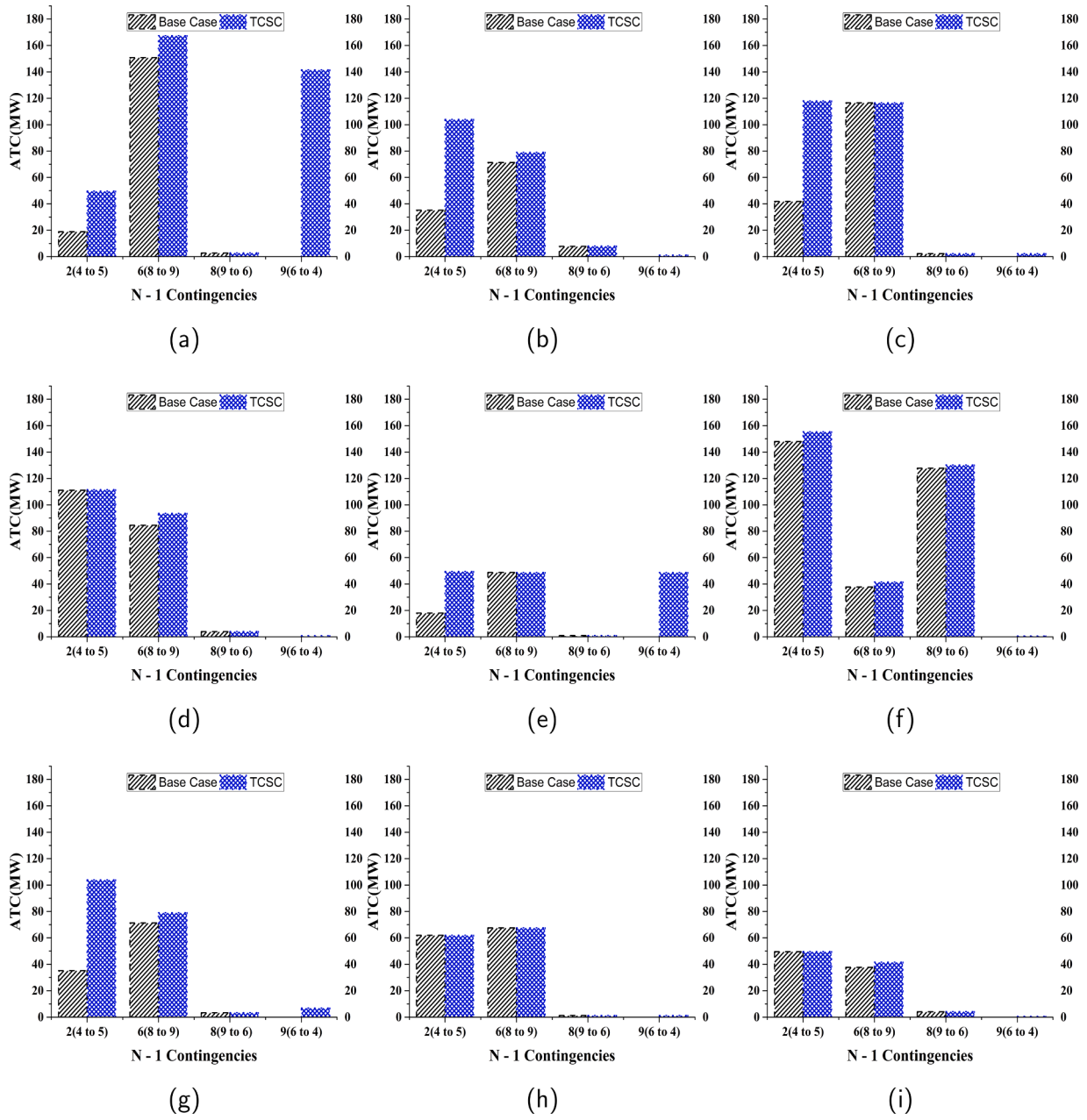

Fig. 10. Power Transfers Under $(N-1)$ for: (a)T1 (b)T2 (c)T3 (d)T4 (e)T5 (f)T6 (g)T7 (h)T8 (i)T9.

Table 6
Single line $(N-1)$ Outage Contingency Ranking.

Line No. (bus i to j)	Cont. Status	PI_S	PI_S Rank	PI_{S-V1}	PI_{S-V2}	PI_{S-V1}	PI_{S-V2} Rank	PI_{S-V1}	PI_{S-V2} Rank
1(1 to 4)	Invalid	NaN	void	NaN	NaN	NaN	void	NaN	void
2(4 to 5)	feasible	0.6302	6	0.265	0	0.8952	5	0.6302	6
3(5 to 7)	unfeasible	1.1672	**1**	0.1808	0	1.3481	**2**	1.1672	**1**
4(2 to 7)	Invalid	NaN	void	NaN	NaN	NaN	void	NaN	void
5(7 to 8)	unfeasible	1.0961	**2**	0.204	0	1.3001	4	1.0961	**3**
6(8 to 9)	feasible	0.6526	5	0.085	0	0.7376	6	0.6526	5
7(9 to 3)	Invalid	NaN	void	NaN	NaN	NaN	void	NaN	void
8(9 to 6)	feasible	0.957	4	0.3675	0	1.3245	**3**	0.957	4
9(6 to 4)	unfeasible	1.0373	**3**	1.4192	0.074	2.4565	**1**	1.1113	**2**
Severe Contingencies		3(5 to 7), 5(7 to 8), 9(6 to 4)		9(6 to 4), 8(9 to 6), 2(4 to 5)	9(6 to 4)	9(6 to 4), 3(5 to 7), 8(9 to 6)		3(5 to 7), 9(6 to 4), 5(7 to 8)	
Credible Contingencies		2(4 to 5), 6(8 to 9), 8(9 to 6)							

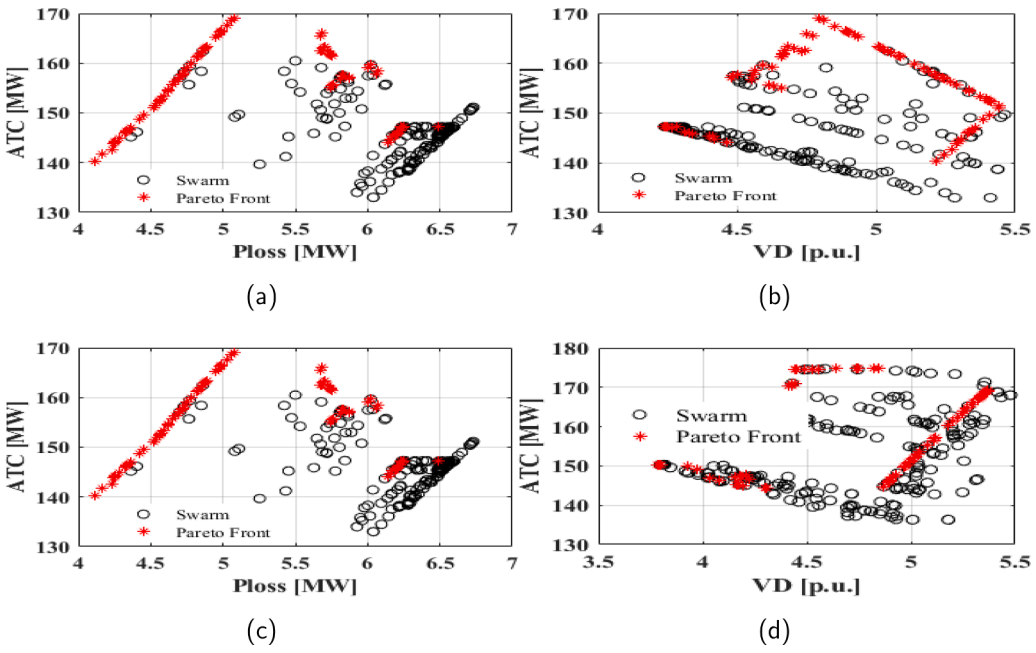

Fig. 11. Slices of Pareto plot for T1 under line 6(8 to 9) outage: (a)$TCSC - DG_{PV}$(b)$TCSC - DG_{PV}$ (c)$TCSC - DG_{PQ}$ (d)$TCSC - DG_{PQ}$.

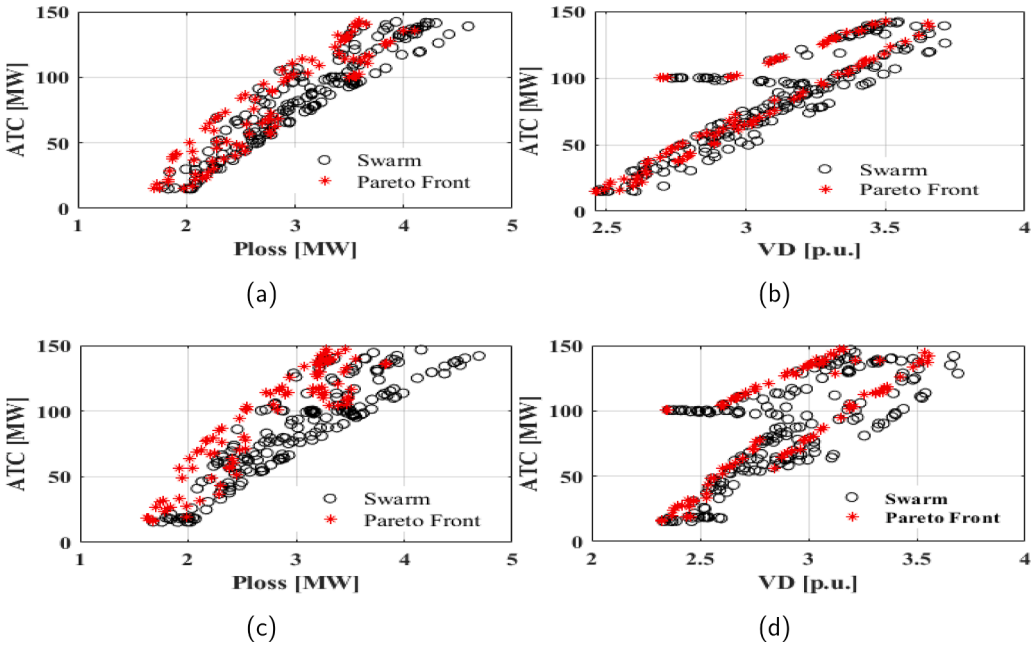

Fig. 12. Slices of Pareto plot for T2 under line 2(4 to 5) outage: (a)$TCSC - DG_{PV}$ (b)$TCSC - DG_{PV}$ (c)$TCSC - DG_{PQ}$ (d)$TCSC - DG_{PQ}$.

a list of severe and credible contingencies considered are obtained.

The ATC enhancement with TCSC was obtained under the credible $(N-1)$ outage contingencies for all power transfer transactions in Table 2. Fig. 10 depicts the impacts of various $(N-1)$ contingencies on the power transfer transactions outlined in Table 2. From Fig. 10a to i observed that the line 9(6 to 4) outage results in zero ATC, which is also consistent with the contingency status of Table 6 caused by the singularity of the base case load flow solution. However, with the optimal deployment of TCSC, for all the transactions, Fig. 10 also depicts enhancement of the ATC above zero under line 9(6 to 4) outage. Furthermore, among the credible contingencies, line 6(8 to 9) outage results in the least ATC value with and without TCSC. Generally, TCSC enhances ATC above base case under all contingencies considered.

Additionally, while the impacts of TSO's contingencies have been illustrated in Fig. 10, DSO resources such as DG reduces the severity of the $(N-1)$ contingency, which is a vital feature of the TSO managed model. Consequently, Figs. 11 to 13 depicts the Pareto front slices of ATC versus Ploss and ATC versus V_D with $TCSC - DG$ coordination under the credible contingencies. From Figs. 11 to 13, compared with TCSC only under contingencies, the ATC, Ploss and V_D were further improved with $TCSC - DG$ coordination. Similar to the cases without contingencies, comparing Fig. 11a and c, Fig. 11b and d, the $TCSC - DG_{PQ}$ under $(N-1)$ obtained superior ATC values than $TCSC - DG_{PV}$. Similar deduction is made with Fig. 13. The Paretor front shapes are similar and specific to transfer directions.

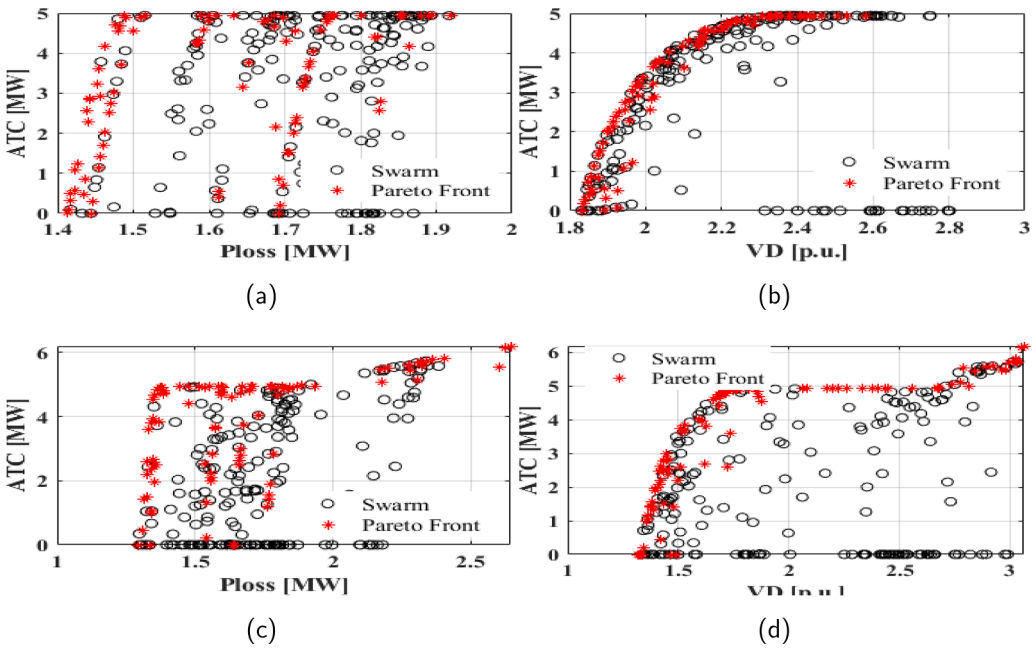

Fig. 13. Slices of Pareto plot for T4 under line 8(9 to 6) outage: (a)$TCSC - DGP_{PV}$ (b)$TCSC - DGP_{PV}$ (c)$TCSC - DG_{PQ}$ (d)$TCSC - DG_{PQ}$.

9. Conclusion

In this paper, a contingency constrained coordination approach of TCSC and DG is developed. The formulated approach is through a multi-level optimization, comprising hybridization of real power flow index and particle swarm optimization in the first level and a multi-objective variant of particle swarm optimization in the second level. Developed approach is also deployed to demonstrate the $TSO - DSO$ coordination through a TSO managed model. Initially, a composite severity index is developed for a contingency constrained coordination of TSO and DSO resources. The developed approach which allows for multiple objectives, account for both the TSO and DSO performance indices. Comparing the results of power transaction with only TCSC and TCSC - DG coordination shows that the DG planning at distribution section in coordination with TCSC reduces the power loss below those of only TCSC. Thus the impact of iT & DN is to ensure that the DSO resource which in this case is the DG, participate in grid service provision in terms of loss reduction. The established correlation among objectives through a Pareto front plot provide deeper insight into the behaviors of Ploss and V_D due to changes in ATC. Compared to the PV model of DG, the PQ model, aside the improvement in ATC, also reduces the power losses. This improvement is attributable to the reactive power supply by the PQ model of DG. The parabolic like shape of the Pareto front indicate that after some maximum ATC values, additional power losses are incurred without a corresponding improvement in the ATC, hence power transfer are not implemented beyond such point.

Declaration of Competing Interest

The authors declare that they have no known competing financial interests or personal relationships that could have appeared to influence the work reported in this paper.

Data availability

Data will be made available on request.

References

[1] M.R. Sindhu, M. Jisma, P. Maya, P. Krishnapriya, M. Vivek Mohan, et al., Optimal placement and sizing of harmonic and reactive compensators in interconnected systems. INDICON 2018 - 15th IEEE India Council International Conference, IEEE, 2018, pp. 1–6, https://doi.org/10.1109/INDICON45594.2018.8987025.

[2] G. Ramesh, T.K. Sunil Kumar, Optimal power flow-based congestion management in restructured power systems, Int. J. Power Energy Convers. 7 (1) (2016) 84–96, https://doi.org/10.1504/IJPEC.2016.075067.

[3] S. Santhanalakshmi, S. Dhivya, Enhancement of power transfer ability in transmission and distribution line using TCSC, Malaya J. Matematik S (2) (2020) 3243–3247, https://doi.org/10.26637/MJM0S20/0834.

[4] A. Singh, A.K. Bohre, Congestion management of system by optimal placement of TCSC in a contingency condition, J. Indian Chem. Soc, WEES 2020 Special Issue 97 (October(B)) (2020) 1–7.

[5] A.A. Sadiq, S.S. Adamu, M. Buhari, Optimal distributed generation planning in distribution networks: a comparison of transmission network models with FACTS, Eng. Sci. Technol.Int. J. 22 (1) (2019) 33–46, https://doi.org/10.1016/j.jestch.2018.09.013.https://linkinghub.elsevier.com/retrieve/pii/S2215098618304555

[6] S. Gumpu, B. Pamulaparthy, A. Sharma, Review of congestion management methods from conventional to smart grid scenario, Int. J. Emerging Electr. Power Syst. 20 (3) (2019) 1–24, https://doi.org/10.1515/ijeeps-2018-0265.

[7] A.A.L. Ahmad, R. Sirjani, Optimal placement and sizing of multi-type FACTS devices in power systems using metaheuristic optimisation techniques: an updated review cumulative gravitational search algorithm opposition gravitational search algorithm, Ain Shams Eng. J. 11 (3) (2020) 611–628, https://doi.org/10.1016/j.asej.2019.10.013.

[8] C. Doddala, V. Suryanarayanareddy, Transmission line congestion management using hybrid fish-bee algorithm with IPFC, Int. Res. J. Eng.Technol. (IRJET) 06 (09) (2019) 2120–2126.

[9] A.A. Sadiq, S.S. Adamu, I. Ndakara, L. Yusuf, et al., Impact of SVC and DG coordination on voltage constrained available transfer capability. 3rd International Engineering Conference (IEC 2019), in: Iec, Federal University of Technology, Minna, Minna, Nigeria, 2019, pp. 615–619.

[10] A.A. Sadiq, S.S. Adamu, M. Buhari, Available transfer capability enhancement with FACTS using hybrid PI-PSO, Turkish J. Electr. Eng.Comput. Sci. 27 (4) (2019) 2881–2897, https://doi.org/10.3906/elk-1812-54.

[11] A.A. Sadiq, M. Buhari, S.S. Adamu, H. Musa, et al., Coordination of multi-type FACTS for available transfer capability enhancement using PI-PSO, IET Gener. Transm. Distrib. 14 (21) (2020), https://doi.org/10.1049/iet-gtd.2020.0886.

[12] A. Fughar, M.N. Nwohu, A.A. Sadiq, J.G. Ambafi, et al., Voltage profile enhancement of the Nigerian North-East 330kV power network using STATCOM, Int. J. Adv. Res.Sci. Eng. Technol. 2 (1) (2015).www.ijarset.com

[13] S. Rakočević, M. Ćalasan, S.H.E. Abdel Aleem, Smart and coordinated allocation of static VAR compensators, shunt capacitors and distributed generators in power systems toward power loss minimization, Energy Sources Part A Recovery Util. Environ. Eff. 00 (00) (2021) 1–19, https://doi.org/10.1080/15567036.2021.1930289.

[14] T. George, A.R. Youssef, S. Kamel, Optimal allocation of DGs and TCSC in radial networks using ant lion optimizer. 2018 20th International Middle East Power

Systems Conference, MEPCON 2018 - Proceedings, IEEE, Cairo University, Egypt, 2019, pp. 1092–1097, https://doi.org/10.1109/MEPCON.2018.8635274.
[15] H. Saberi, S. Mehraeen, B. Wang, Stability improvement of microgrids using a novel reduced UPFC structure via nonlinear optimal control. 2018 IEEE Applied Power Electronics Conference and Exposition (APEC), IEEE, San Antonio, TX, USA, 4–8 March 2018, 2018, pp. 3294–3300, https://doi.org/10.1109/APEC.2018.8341575.
[16] T. Alsuwian, A. Basit, A.A. Amin, M. Adnan, M. Ali, An optimal control approach for enhancing transients stability and resilience in super smart grids enhanced reader.pdf, Electronics (Basel) 11 (3236) (2022) 1–38, https://doi.org/10.3390/electronics11193236.
[17] M. Pandya, J.G. Jamnani, Transient stability assessment by coordinated control of SVC and TCSC with particle swarm optimization, Int. J. Eng. Adv. Technol. 9 (1) (2019) 2506–2510, https://doi.org/10.35940/ijeat.F8144.109119.
[18] M. Aybar-Mejia, J. Batista, K. Diaz, W. Fernandez, F. Reyes-Romero, L.-C. De E, D. Mariano-Hernandez, Reduction of operational restrictions of the transmission system in electrical systems through facts implementation, e-Prime - Adv Electr. Eng.Electron. Energy 2 (100047) (2022) 1–8, https://doi.org/10.1016/j.prime.2022.100047.
[19] B. Singh, V. Mukherjee, P. Tiwari, GA-based optimization for optimally placed and properly coordinated control of distributed generations and static var compensator in distribution networks, Energy Rep. 5 (2019) 926–959, https://doi.org/10.1016/j.egyr.2019.07.007.
[20] M. Santamouris, K. Vasilakopoulou, Present and future energy consumption of buildings: challenges and opportunities towards decarbonisation, e-Prime - Adv. Electr. Eng.Electron. Energy 1(100002) (August) (2021) 1–14, https://doi.org/10.1016/j.prime.2021.100002.
[21] M. Shafiul Alam, F.S. Al-Ismail, A. Salem, M.A. Abido, et al., High-level penetration of renewable energy sources into grid utility: challenges and solutions, IEEE Access 8 (2020) 190277–190299, https://doi.org/10.1109/ACCESS.2020.3031481.
[22] J.A.P. Lopes, N. Hatziargyriou, J. Mutale, P. Djapic, N. Jenkins, et al., Integrating distributed generation into electric power systems: a review of drivers, challenges and opportunities, Electr. Power Syst. Res. 77 (9) (2007) 1189–1203, https://doi.org/10.1016/j.epsr.2006.08.016.
[23] Y. Zhang, Y. Xu, H. Yang, Y.Z. Dong, et al., Voltage regulation-oriented co-planning of distributed generation and battery storage in active distribution networks, Electr. Power Energy Syst. 105 (2019) 79–88, https://doi.org/10.1016/j.ijepes.2018.07.036.
[24] O.A.C. De Koster, J.A. Domínguez-Navarro, Multi-objective tabu search for the location and sizing of multiple types of FACTS and DG in electrical networks, Energies 13 (11) (2020), https://doi.org/10.3390/en13112722.
[25] F. Ugranli, E. Karatepe, Coordinated TCSC allocation and network reinforcements planning with wind power, IEEE Trans. Sustain. Energy 8 (4) (2017) 1694–1705, https://doi.org/10.1109/TSTE.2017.2702105.
[26] M. Bolfek, T. Capuder, An analysis of optimal power flow based formulations regarding DSO-TSO flexibility provision, Int. J. Electr. PowerEnergy Syst. 131 (January) (2021) 106935, https://doi.org/10.1016/j.ijepes.2021.106935.
[27] Z. Lubric, H. Pandzic, M. Carrión, Transmission expansion planning model considering battery energy storage, TCSC and lines using AC OPF, IEEE Access 8 (2020) 203429–203439, https://doi.org/10.1109/ACCESS.2020.3036381.
[28] H. Abdel-Mawgoud, S. Kamel, M. Khasanov, T. Khurshaid, A strategy for PV and BESS allocation considering uncertainty based on a modified Henry gas solubility optimizer, Electr. Power Syst. Res. 191 (October 2020) (2021) 106886, https://doi.org/10.1016/j.epsr.2020.106886.
[29] D.A. Contreras, K. Rudion, Computing the feasible operating region of active distribution networks: comparison and validation of random sampling and optimal power flow based methods, IET Gener. Transm. Distrib. 15 (10) (2021) 1600–1612, https://doi.org/10.1049/gtd2.12120.
[30] S.Y. Hadush, L. Meeus, DSO-TSO cooperation issues and solutions for distribution grid congestion management, Energy Policy 120 (December 2017) (2018) 610–621, https://doi.org/10.1016/j.enpol.2018.05.065.
[31] H. Le, I. Mezghani, A. Papavasiliou, A game-theoretic analysis of transmission-distribution system operator coordination R, Eur. J. Oper. Res. 274 (1) (2019) 317–339, https://doi.org/10.1016/j.ejor.2018.09.043.
[32] L. Lind, R. Cossent, J.P. Chaves-Ávila, T. Gómez San Román, Transmission and distribution coordination in power systems with high shares of distributed energy resources providing balancing and congestion management services, Wiley Interdiscip. Rev. EnergyEnviron. 8 (6) (2019) 1–19, https://doi.org/10.1002/wene.357.
[33] S. Stanković, L. Söder, Z. Hagemann, C. Rehtanz, Reactive power support adequacy at the DSO/TSO interface, Electr. Power Syst. Res. 190 (April 2020) (2021), https://doi.org/10.1016/j.epsr.2020.106661.
[34] M.A. El-Meligy, M. Sharaf, A.T. Soliman, A coordinated scheme for transmission and distribution expansion planning: a Tri-level approach, Electr. Power Syst. Res. 196 (April) (2021), https://doi.org/10.1016/j.epsr.2021.107274.
[35] D. Rashmi, S. Sivasubramani, A game theoretic approach for profit allocation considering DG and FACTS devices. 2021 IEEE 2nd International Conference on Smart Technologies for Power, Energy and Control (STPEC), 2021, pp. 1–6, https://doi.org/10.1109/STPEC52385.2021.9718660.
[36] V. Kohan, Z. Conka, M. Kolcun, Impact of TCSC on generator operation. CANDO-EPE 2020 - Proceedings, IEEE 3rd International Conference and Workshop in Obuda on Electrical and Power Engineering, IEEE, Budapest, Hungary, 2020, pp. 131–136, https://doi.org/10.1109/CANDO-EPE51100.2020.9337797.
[37] W. Liu, X. Yang, T. Zhang, A. Abu-Siada, Multi-objective optimal allocation of TCSC for power systems with wind power considering load randomness, J. Electr. Eng. Technol. (2022), https://doi.org/10.1007/s42835-022-01233-w.
[38] I.M. Wartana, N.P. Agustini, Optimal integration of series and shunt FACTS with Wind energy for active power loss reduction, in: P.A.M. Nahhas, P.A.A. Ibhadode (Eds.), Renewable Energy - Recent Advances, IntechOpen, Rijeka, 2022, https://doi.org/10.5772/intechopen.107296.
[39] K. Dwarakesh, Enhancement of power transfer ability in transmission and distribution line using TCSC, Malaya J. Metematic S (2) (2020) 2542–2546.
[40] A.G. Givisiez, K. Petrou, L.F. Ochoa, A review on TSO-DSO coordination models and solution techniques, Electr. Power Syst. Res. 189 (October 2019) (2020) 106659, https://doi.org/10.1016/j.epsr.2020.106659.
[41] S. Massucco, P. Pongiglione, F. Silvestro, M. Paolone, F. Sossan, et al., Siting and Sizing of Energy Storage Systems: towards a unified approach for transmission and distribution system operators for reserve provision and grid support. 21st Power Systems Computation Conference Power Systems Computation Conference, PSCC 2020, Porto, Portugal, 2020, pp. 1–8, https://doi.org/10.1016/j.epsr.2020.106660.
[42] H. Gerard, E.I. Rivero Puente, D. Six, Coordination between transmission and distribution system operators in the electricity sector: a conceptual framework, Util. Policy 50 (2018) 40–48, https://doi.org/10.1016/j.jup.2017.09.011.
[43] A. Hermann, T.V. Jensen, J. Østergaard, J. Kazempour, et al., A complementarity model for electric power transmission-distribution coordination under uncertainty, Eur. J. Oper. Res. (2021), https://doi.org/10.1016/j.ejor.2021.08.018.
[44] R. Jain, Y. Nag, K. Prabakar, M. Baggu, K. Schneider, et al., Modern trends in power system protection for distribution grid with high DER penetration, e-Prime - Adv. Electr. Eng.Electron. Energy 2 (October) (2022) 1–16, https://doi.org/10.1016/j.prime.2022.100080.
[45] R. Ansaripour, H. Barati, A. Ghasemi, Multi-objective chance-constrained transmission congestion management through optimal allocation of energy storage systems and TCSC devices, Electr. Eng. 104 (6) (2022) 4049–4069, https://doi.org/10.1007/s00202-022-01599-0.
[46] P. Manohar, P. Rajesh, F.H. Shajin, A comprehensive review of congestion management in power system, Int. J. Integr. Eng. 14 (6) (2022) 346–362, https://doi.org/10.30880/ijie.2022.14.06.030.http://penerbit.uthm.edu.my/ojs/index.php/ijie
[47] Z.M. Ali, H.M. Hasanien, C. Martin, E.M. Ahmed, S. Rakoc, R.A. Turky, S.H. E. Abdel, BONMIN solver-based coordination of distributed FACTS compensators and distributed generation units in modern distribution networks, Ain Shams Eng. J. 13 (101664) (2022) 1–17, https://doi.org/10.1016/j.asej.2021.101664.
[48] A.S. Siddiqui, P. Baredar, Optimal location and sizing of conglomerate DG-FACTS using an artificial neural network and heuristic probability distribution methodology for modern power system operations, Prot. Control Mod. Power Syst. 7 (9) (2022) 1–25, https://doi.org/10.1186/s41601-022-00230-5.
[49] S. Ghaedi, B. Tousi, M. Abbasi, M. Alilou, et al., Optimal placement and sizing of TCSC for improving the voltage and economic indices of system with stochastic load model, J. Circuits Syst. Comput. 29 (13) (2020) 1–21, https://doi.org/10.1142/S0218126620502175.
[50] S. Galvani, B. Mohammadi-Ivatloo, M. Nazari-Heris, S. Rezaeian-Marjani, et al., Optimal allocation of static synchronous series compensator (SSSC) in wind-integrated power system considering predictability, Electr. Power Syst. Res. 191 (September 2020) (2021) 106871, https://doi.org/10.1016/j.epsr.2020.106871.
[51] A.G. Givisiez, K. Petrou, L.F. Ochoa, A review on TSO-DSO coordination models and solution techniques, Electr. Power Syst. Res. 189 (2020), https://doi.org/10.1016/j.epsr.2020.106659.
[52] L. Jebaraj, S. Sakthivel, A new swarm intelligence optimization approach to solve power flow optimization problem incorporating conflicting and fuel cost based objective functions, e-Prime - Adv. Electr. Eng.Electron. Energy 2 (100031) (November 2021) (2022) 1–36, https://doi.org/10.1016/j.prime.2022.100031. https://app.dimensions.ai/details/publication/pub.1146080376
[53] N.S. Rao, J. Amarnath, V.P. Rao, Comparison for performance of multitype FACTS devises on available transfer capability in a deregulated power system. 2014 International Conference on Smart Electric Grid, ISEG 2014, 2014, https://doi.org/10.1109/ISEG.2014.7005611.
[54] B. Mahdad, K. Srairi, Adaptive differential search algorithm for optimal location of distributed generation in the presence of SVC for power loss reduction in distribution system, Eng. Sci. Technol.Int. J. 19 (3) (2016) 1266–1282, https://doi.org/10.1016/j.jestch.2016.03.002.
[55] S. Jahan, A.M. Mannan, Voltage stability analysis of a 16-bus distribution network based on voltage sensitivity factor, Int. J. Multidiscip. Sci. Eng. 5 (4) (2014) 1–5.
[56] A.S.O. Ogunjuyigbe, T.R. Ayodele, O.O. Akinola, Impact of distributed generators on the power loss and voltage profile of sub-transmission network, J. Electr. Syst. Inf. Technol. 3 (1) (2016) 94–107, https://doi.org/10.1016/j.jesit.2015.11.010.
[57] C. Ma, P. Kaufmann, J.C. Töbermann, M. Braun, et al., Optimal generation dispatch of distributed generators considering fair contribution to grid voltage control, Renew. Energy 87 (2016) 946–953, https://doi.org/10.1016/j.renene.2015.07.083.
[58] N.S. Vadivoo, S.M.R. Slochanal, Distribution system restoration using genetic algorithm with distributed generation, Mod. Appl. Sci. 3 (4) (2009) 98–110, https://doi.org/10.5539/mas.v3n4p98.http://www.ccsenet.org/journal/index.php/mas/article/view/1258
[59] N.G.A. Hemdan, M. Kurrat, Efficient integration of distributed generation for meeting the increased load demand, Int. J. Electr. PowerEnergy Syst. 33 (9) (2011) 1572–1583, https://doi.org/10.1016/j.ijepes.2011.06.032.
[60] E.S. Ali, S.M.A. Elazim, A.Y. Abdelaziz, Ant lion optimization algorithm for optimal location and sizing of renewable distributed generations, Renew. Energy 101 (2017) 1311–1324, https://doi.org/10.1016/j.renene.2016.09.023.
[61] S.A. Chithradevi, L. Lakshminarasimman, R. Balamurugan, Stud krill herd algorithm for multiple DG placement and sizing in a radial distribution system,

Eng. Sci. Technol.Int. J. 20 (2) (2017) 748–759, https://doi.org/10.1016/j.jestch.2016.11.009.
[62] A.A. Hassan, F.H. Fahmy, A.A. Nafeh, M.A. Abuelmagd, Genetic single objective optimisation for sizing and allocation of renewable DG systems, Int. J. Sustain. Energy 6451 (October) (2015) 0–18, https://doi.org/10.1080/14786451.2015.1053393.
[63] M. Balasubbareddy, S. Sivanagaraju, C. Venkata, A non-dominated sorting hybrid cuckoo search algorithm for multi-objective optimization in the presence of FACTS devices, Russian Electr. Eng. 88 (1) (2017) 44–53, https://doi.org/10.3103/S1068371217010059.
[64] C.a. Canizares, A. Berizzi, P. Marannino, Using FACTS controllers to maximize available transfer capability. Proceedings of the Bulk Power Systems Dynamics and Control IV-Restructuring, Santorini, Greece, 1998, pp. 633–641.https://pdfs.semanticscholar.org/0769/616c0e46c993e239b60b0321c9e7454aa0b6.pdf.

Ahmad Abubakar Sadiq received Bachelors of Engineering degree in Electrical and Computer Engineering, and Masters of Engineering in Electrical Power and Machines, both from the Federal University of Technology, Minna, Nigeria. He holds a Doctoral degree in Electrical Engineering from Bayero University, Kano Nigeria. He is a member of IEEE and COREN registered Electrical Engineer with skills and experience in steady-state modelling of power systems and components such as Distributed Generation (DG) and FACTS. His interest is in power systems planning, operations and optimization, with Distributed Generation Integration and FACTS deployment for transfer capability improvement. He has participated in international projects/grants such as the improvement of Continuation Power Flow (CPF) algorithm in MATPOWER in collaboration with Power Systems Engineering Research Centre (PSERC) Cornel University, Ithaca, NY; Artificial Intelligence for Clean Energy (AI4CE) Development, funded by the Royal Academy of Engineering UK. He has published in reputable journals and conferences which are widely cited by the literal community.

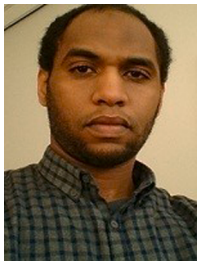

Muhammad Buhari received the BEng and MEng degrees in Electrical Engineering from Bayero University, Kano, Nigeria, in 2006 and 2011, respectively, and the M.Sc. degree in entrepreneurship and Electrical and Electronics Engineering from the University of Nottingham, U.K., in 2010. He received the PhD degree from the University of Manchester, U.K., 2016. He currently works at the Department of Electrical Engineering and the Centre for Renewable Energy Research at Bayero University, Kano, Nigeria. Muhammad does research in Integration of Renewable energy systems and new technologies into conventional power networks. Their current project is 'Power Transfer Capability Enhancement of Transmission Grid with FACTS and DG and also Integration of Energy Storage into the Nigerian distribution networks.

James Garba Ambafi Obtained BEng in Electrical and Electronics Engineering from the Federal University of Technology Yola, Nigeria, MEng degree in Electrical Power and Machines from Federal University of Technology Minna, Nigeria, and a PhD degree in Electrical Engineering at Bayero University, Kano, Nigeria. He is currently a Senior Lecturer at the Department of Electrical & Electronics Engineering, Federal University of Technology, Minna. Nigeria. His research interests include; Power System Stability and Control, hybrid renewable energy systems, energy management in hybrid systems, Demand Side management, rural healthcare power development and optimization techniques for renewable energy (RE) integration. He has published in Journals of high repute.

Sunusi Sani Adamu holds PhD in Electrical Engineering from Bayero University Kano, in 2008, MSc in Electrical Power and Machines from Ahmadu Bello University Zaria in 1996, and a BEng Electrical Engineering from Bayero University in 1985. He is a full Professor of Electrical Engineering in the Department of Electrical Engineering, Bayero University Kano, Nigeria. He has mentored and supervised several academics at both PhD and MEng level. His area of specialization is in Power Systems Stability and Control.

Mark N. Nwohu received his bachelor of Engineering (BEng) in Power Systems Engineering Technology from Federal University of Technology, Owerri, Nigeria, in 1988. He got his Master's degree in Power and Machines from University of Benin, Nigeria in 1994. In 2007, he badged on his Doctor of Philosophy (PhD) Degree in Power Systems Engineering from Abubakar Tafawa Balewa University, Bauchi, Nigeria. His research interest includes Power System Analysis, Power System Stability and Control, Application of FACTS devices and Artificial Intelligence to Power Systems, System Simulation, Power Quality, and Numerical Analysis. He is a Professor of Electrical Power Systems Engineering at the Federal University of Technology, Minna, Niger State, Nigeria. He is a registered, practicing Engineer with the Council for the Regulation of Engineering in Nigeria (COREN), and a member of IAENG, IET, IEEE, NSE and ISDS. He is an author of over fifty (60) published articles in reputable National and International journals.